

RSC Advances

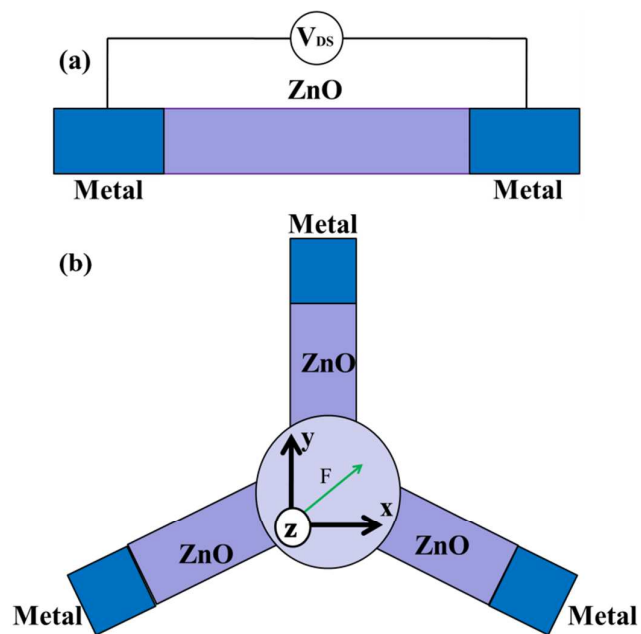


This is an *Accepted Manuscript*, which has been through the Royal Society of Chemistry peer review process and has been accepted for publication.

Accepted Manuscripts are published online shortly after acceptance, before technical editing, formatting and proof reading. Using this free service, authors can make their results available to the community, in citable form, before we publish the edited article. This *Accepted Manuscript* will be replaced by the edited, formatted and paginated article as soon as this is available.

You can find more information about *Accepted Manuscripts* in the [Information for Authors](#).

Please note that technical editing may introduce minor changes to the text and/or graphics, which may alter content. The journal's standard [Terms & Conditions](#) and the [Ethical guidelines](#) still apply. In no event shall the Royal Society of Chemistry be held responsible for any errors or omissions in this *Accepted Manuscript* or any consequences arising from the use of any information it contains.



ZnO nanotetrapods could be designed as multiterminal strain sensors for enhancing sensitivity and directivity.

Piezoelectric effect of 3-D ZnO nanotetrapods

Bing Yin^{1,2}, Yu Qiu^{1,2}, Heqiu Zhang^{1,2}, Jixue Lei^{1,2}, Yue Chang^{1,2}, Jiuyu Ji¹, Yingmin

Luo¹, Yu Zhao¹, Lizhong Hu^{1,2 a)}

¹*School of Physics and Optoelectronic Technology, Dalian University of Technology, Dalian 116024, China*

²*The Key Laboratory for Micro/Nano Technology and System of Liaoning Province, Dalian University of Technology, Dalian 116024, People's Republic of China*

Abstract

In this work the piezoelectric effect of 3-D ZnO nanotetrapods (ZNTs) is studied by the finite element method. The results show that the nanogenerator based on ZnO nanotetrapods has a number of advantages over the generators based on traditional hexagonal nanorods due to the unique tetrapod structure. Different from double-terminal sensors, the sensors based on ZnO nanotetrapods can give multiple responses to a single signal at the same time. Therefore, ZnO nanotetrapods could be designed as multiterminal strain sensors for enhancing sensitivity and directivity. Here we demonstrate that lateral bending of ZnO nanotetrapods (ZNTs) results in higher output piezopotentials than vertical compression. Effect of geometric size on piezopotential is also studied. The results provide guidance for optimizing the output of piezoelectric nanogenerators and designing high-performance strain sensors .

1. Introduction

In recent decades, significant and rapid development has been made in nanotechnology which facilitates various interesting nanoscale applications such as sensors¹, actuators^{2, 3}, piezo-phototronics⁴ and piezo-controlled chemical reactions⁵. Nanoscale semiconducting crystalline structures, due to their unusual optical and electrical properties, have been widely studied. Among the various materials, as a wide bandgap semiconductor with large excitation energy of 60meV at room temperature, zinc oxide (ZnO) has aroused a wide range of research interests because of its excellent physical properties.

Since Wang and Song's pioneering work⁶ on the first nanogenerator prototype using piezoelectric nanowires for converting mechanical energy into electricity, there has been an increasing interest in investigating various technologies, including theoretical calculations and experimental characterization methods⁷⁻¹⁰, to promote the development of self-powered piezoelectric nanostructures. An impressive variety of ZnO crystal morphologies have been synthesized, for example, ZnO nanowires¹¹⁻¹³, nanosheets¹⁴, nanotubes¹⁵⁻¹⁹, nanobelts²⁰⁻²⁵, nanorods²⁶⁻²⁹, nanowalls³⁰, nanotapers³¹⁻³³. ZnO nanotetrapods, consisting of a polyhedron-shaped zinc blende-structured “core” with four needle or rod-shaped wurtzite-structured legs protruding out at tetrahedral angles³⁴, are of particular interest due to their unique nanoscale three-dimensional (3D) architectures that can deliver the functions of delicate multiterminal nanodevices³²⁻³⁶. Due to their novel structure with an occupied 3-D tetrahedral space and ease of synthesis with controllable size and shape, ZnO nanotetrapods have been extensively studied in the areas of field effect transistors³⁷, gas sensors³⁸, UV detectors³⁵, p-n junction diodes³³, logic switches³⁹ and Schottky photodiodes⁴⁰. However, few studies have been conducted on the piezoelectric effect of nanotetrapods for strain sensors or nanogenerators.

In this paper, we use the finite element method (FEM, COMSOL) for estimating the piezopotential of the three-dimensional ZnO nanotetrapods(ZNTs). The size related energy harvesting ability is also predicted by comparing with the same size ZnO

hexagonal nanorods (ZHNRs). The result suggests that in the case of lateral bend the absolute value of piezopotential is proportional to the external force or length of the ZNTs but inversely proportional to edge. In the case of vertical compression the absolute value of piezopotential is proportional to length but inversely proportional to edge. In particular, theoretical calculations¹⁰ and experiment work⁴¹ have shown that vertical compression may be better than lateral bending from both the points of view of high output voltages and mechanical-to-electrical energy transduction capabilities. However, by using FEM calculation, we confirm that lateral bending of ZNTs results in higher piezopotentials than vertical compression. It means that bending is likely more effective for energy harvesting than vertical compression for ZNTs. And laterally bending ZNTs can actually be ideal for transducing minuscule mechanical forces into high and accessible piezopotentials rather than ZHNRs. Moreover, we show that, ZnO nanotetrapods have a number of advantages over traditional hexagonal nanorods for nanogenerators and sensors in terms of efficiency, stability and robustness. Our results can provide guidelines for designing high-performance piezo-nano-devices for piezotronics, piezo-phototronics, piezo-controlled chemical reactions, as well as for the electro-mechanical characterization of piezoelectric nanostructures.

2. Simulation method

Using the finite element method, the piezopotential of a fully coupled electro-mechanical system of nanostructure is calculated from the piezo-electric coupled equations^{42,43}. According to the conventional theory of piezoelectricity and elasticity, the constituter equations can be written as E_k

$$\begin{cases} \sigma_p = c_{pq}\varepsilon_q - e_{kp}E_k \\ D_i = e_{iq}\varepsilon_q + k_{ik}E_k \end{cases} \quad (1)$$

Where ε_q and σ_p are the strain and stress tensor, respectively. e_{kp} , k_{ik} , and D_i are the linear piezoelectric coefficient, dielectric constant, and electric displacement, respectively. e_{iq} is the transpose of e_{kp} .

For simplicity of the calculation, the ZNT is assumed to be intrinsic. The legs of the

nanotetrapod are hexagonal nanorods, three of which are fixed and electrically grounded. In our previous experiments, it was also found that the diameter and length of nanostructure could be adjusted by controlling the reaction time, temperature and gas pressure. Unless otherwise noted, the dimensions of the nanostructure are as follows: the edge, E_T , and length, L_T , for the legs of the ZNT, equal to $0.6\mu\text{m}$ and $15\mu\text{m}$, respectively, the total height of the ZNT is $20.8\mu\text{m}$. And the edge, E_h , and length, L_h , for the hexagonal nanorods (ZHNR), also equal to $0.6\mu\text{m}$ and $20.8\mu\text{m}$, respectively. In all our simulations, the nanostructures are laterally deflected or vertically compressed by a force which is uniformly applied at the entire top surface of the leg; the magnitude of the lateral bending or vertical compressive force is 80nN . ZnO nanotetrapod is a structure owing to the co-existence of two ZnO phases: cubic and wurtzite. ZnO nanotetrapod has the cubic phase at the core, and four legs with [0001] wurtzite structure extending along the [111] of the cubic structure³⁴. According to the unique 3-D structure, the c-axis of the crystal was along the direction of the legs growth. The material's constants of ZnO are the elastic constants: $c_{11} = 207\text{ GPa}$, $c_{12} = 117.7\text{ GPa}$, $c_{13} = 106.1\text{ GPa}$, $c_{33} = 209.5\text{ GPa}$, $c_{44} = 44.8\text{ GPa}$, $c_{55} = 44.6\text{ GPa}$; piezoelectric constants $e_{15} = 0.45\text{ C/m}^2$, $e_{31} = 0.51\text{ C/m}^2$, $e_{33} = 1.22\text{ C/m}^2$; relative dielectric constants $k_{\perp} = 7.77$, $k_{\parallel} = 8.9$, respectively.

3. Results and discussion

3.1 Lateral bending

The output piezopotential is the major criteria for designing nanogenerator. To demonstrate the energy harvesting ability, the piezopotential of the ZNT is predicted by comparing with the same size ZnO hexagonal nanorods (ZHNRs). The calculated piezopotential distributions in the bent nanostructure are revealed in Fig.1 (Fig.1(a) and (b), the side view; Fig.1(c) and (d), the top view). The piezopotential in the tensile area is positive and that in the compressive area is negative, and they are antisymmetric along the Y-axis. Importantly, the maximum piezopotential of the ZNT is -1.1639V , which is approximately 4-fold higher voltage by comparison to the hexagonal nanorod ($\sim -0.2753\text{V}$). It's worth noting that the displacement of the

ZHNR is $0.2349\mu\text{m}$ which is twice as the displacement of the ZNT ($0.1295\mu\text{m}$). The structure brings the advantage of lower strain on legs and a higher piezopotential.

There are two reasons for the much higher piezopotentials found in the ZNTs: first, in comparison with the hexagonal nanorods (ZHNRs), the ZNTs mechanically allows one to generate much higher strains at the core but lower strains at the legs. Second, because the high-strain region (the core) is far from the bottom contact, its strain can be effectively converted into a piezopotential. As a result, the magnitude of the piezopotential in the ZNT is much higher. A piezoelectric nanostructure for energy harvesting must necessarily include two electrical contacts to be connected to the load¹⁰. Thus, the dimension and position of the electrical contacts are important. The minimum and maximum values of the piezopotential in the deflected ZHNRs are found in very small and internal portions as shown in Fig.1 (b). The minimum and maximum values of the piezopotential are not accessible from outside contacts. However, this problem is absent in the ZNTs; the minimum and maximum values of the piezopotential in the deflected ZNTs are found in different legs as shown in fig.1(a),(c), which offers important practical advantages to connect to an external circuit. Moreover, the free leg of the ZNT is laterally deflected and other below legs are connected to electrodes. It is crucial for sophisticated sensors for microenvironment detection with one free terminal inserted³⁴. The nanotetrapods can ensure strong practicability for building high-efficiency piezoelectric nanogenerators.

3.2 Strain sensors based on the bent ZNTs

Fig. 2 shows the schematic plans of the designed sensors based on the ZHNR and ZNT. It can be seen that the tetrapod devices are obviously different from those devices based on a single nanowire/nanotube. They have three terminals connected to electrodes, respectively and the top leg is used as receiving terminal for detecting mechanical stimulation signal. The electrical properties between every two terminals could be characterized, respectively. The calculated piezopotential distributions in the ZNTs bent by a force (80nN) from different directions are revealed and viewed from the top (Fig.3 (a)-(d)). As shown in Fig.3 the distribution of piezopotential in the ZNT is largely determined by the direction and magnitude of the force. The strain sensors

based on the ZNT could simultaneously give two responses to a single outside signal at the same time. Thus the strain sensors based on the ZNT can be regarded as two individual two terminal sensors being assembled together. The two simultaneous responses can be referred to each other. This can help to detect the direction and magnitude of the force. This means that the ZNTs could be designed as multiterminal sensors for enhancing sensitivity and directivity.

3.3 Effect of geometric size on piezopotential

Using our model, we studied the distributions of the piezopotential under various forces from 50nN to 90 nN. For the same edge ($0.6\mu\text{m}$) and length ($15\mu\text{m}$) of the legs, the piezopotential increases almost linearly with the enhancing of force as shown in Fig.4 (a). As mentioned above, the X axis represents the length of the legs of the ZNT; for instance, when the x equals $15\mu\text{m}$, it means the length of each leg is $15\mu\text{m}$ and, accordingly, the total height of the ZNT/ ZHNR is $20.8\mu\text{m}$. Fig.4 (b), (c) show the piezopotential as a function of edge and length of the ZNTs and ZHNRs under lateral force 80nN. The piezopotential increases with the increasing of the length, but decreases with the increasing of the edge. As shown in Fig.4 (b) and (c), compared with ZnO hexagonal nanorods (ZHNR), ZnO nanotetrapods (ZNTs) obtained much higher piezopotentials. The ZNTs offer superior mechanical robustness, including a much stably adhesion to the substrate, and is less subject to stain, which is a key for efficient mechanical-to-electrical transduction.

3.4 Vertical compression

In case of vertical compression, the piezopotential at the top is negative, which is in agreement with the nanorods. The piezopotential increases almost linearly with the enhancing of force as shown in Fig.4 (d). When a ZNT is vertically and uniformly compressed with a force (80nN) at the top, the generated piezopotential is proportional to the length of the legs and is also dependent on its cross-section dimension. The corresponding potential variation curves are given in Fig.4 (e) and (f), respectively. Generally speaking, vertical compression is likely more effective for 1-D nanostructure to harvest energy⁴⁴. However, it is difficult to achieve because the possibility of vertical compression of an 1-D nanostructure is severely compromised

by the rigid top electrode and the verticality of the nanostructure⁴⁵, which may limit the scope of applications (for example, flexible piezoelectric nanogenerators). For the ZNTs, lateral bending is more effective to obtain higher output piezopotentials. Comparing between Fig.4 (a) and (d), (b) and (e), as well as (c) and (f), it is clearly demonstrated that laterally bending a ZNT, the generated piezopotential will be much larger than that generated by a same magnitude of vertical compression. Therefore, by applying a bending force, the electricity generation capacity of the piezoelectric generators based on ZNTs can be greatly improved. Many nanowire generators were based on 1-D piezoelectric nanorods which were attached to a substrate at one end and were free to move at the other end. However, there were problems with the output stability, mechanical robustness, lifetime and environmental adaptability of such devices. As the external forces applied and released, there will be a relative scrubbing and sliding between the top electrode and the nanowires, which may result in wearing and increased contact resistance/instability. Thus, the mechanical properties of nanorods are critical to the durability of the piezoelectric nanogenerators. Due to the force is applied to the free leg, the nanogenerator based on a nanotetrapods that is firmly attached to metal electrodes at the below legs does not involve sliding contacts. Because the force is applied at the top free leg, there is not rubbing together of the electrode and ZNTs. It is crucial to provide stable and reliable electrical contacts.

3. Conclusions

In summary, piezoelectric effect of ZnO nanotetrapods has been studied by FEM. The results indicate that lateral bending is likely not optimal for energy harvesting; however, lateral bending of ZnO nanotetrapods may be ideal for nanogenerators or sensors. The nanogenerators based on ZnO nanotetrapods have a number of advantages over the generators based on traditional hexagonal nanorods in terms of efficiency, stability and robustness. The strain sensors based on the ZnO nanotetrapods could simultaneously give two responses to a single outside signal at the same time, which means that the ZNTs could be designed as multiterminal sensors for enhancing sensitivity and directivity. Furthermore, the calculated function between

the geometry size and piezopotential also provides guidelines for designing high-performance strain sensors or nanogenerators by adjusting geometric size.

Acknowledgements

This work was supported by the Fundamental Research Funds for the Central Universities (DUT14LK35), Foundation of Key laboratory for Micro/Nano Technology and System of Liaoning Province (20140405), the Fundamental Research Funds for the Central Universities (Project No.DUT11LK46), the Doctoral Project by the China Ministry of Education (Project No.20070141038), and Open Fund by Laboratory for MEMS, Liaoning Province.

References

1. M. R. Alenezi, T. H. Alzanki, A. M. Almeshal, A. S. Alshammari, M. J. Beliatis, S. J. Henley and S. R. P. Silva, *Rsc Adv*, 2014, 4, 49521-49528.
2. S. H. Lee, S. S. Lee, J. J. Choi, J. U. Jeon and R. Ko, *Key Eng Mat*, 2004, 270-273, 1095-1100.
3. S. O. Catarino, L. R. Silva, P. M. Mendes, J. M. Miranda, S. Lanceros-Mendez and G. Minas, *Sensor Actuat B-Chem*, 2014, 205, 206-214.
4. Z. L. Wang, *Adv Mater*, 2012, 24, 4632-4646.
5. M. B. Starr, J. Shi and X. D. Wang, *Angew Chem Int Edit*, 2012, 51, 5962-5966.
6. Z. L. Wang and J. H. Song, *Science*, 2006, 312, 242-246.
7. Z. L. Wang, *Materials Science and Engineering: R: Reports*, 2009, 64, 33-71.
8. Y. Gao and Z. L. Wang, *Nano Lett*, 2007, 7, 2499-2505.
9. B. Tian, X. Zheng, T. J. Kempa, Y. Fang, N. Yu, G. Yu, J. Huang and C. M. Lieber, *Nature*, 2007, 449, 885-889.
10. C. Falconi, G. Mantinia, A. D'Amico and Z. L. Wang, *Sensor Actuat B-Chem*, 2009, 139, 511-519.
11. S. Lee, R. Hinchet, Y. Lee, Y. Yang, Z. H. Lin, G. Ardila, L. Montes, M. Mouis and Z. L. Wang, *Adv Funct Mater*, 2014, 24, 1163-1168.
12. C. W. Huang, J. Y. Chen, C. H. Chiu and W. W. Wu, *Nano Lett*, 2014, 14, 2759-2763.
13. D. Zappa, E. Comini and G. Sberveglieri, *Nanotechnology*, 2013, 24, 444008-444016.
14. S. Alimirsalari, F. Tajabadi, S. M. Salehkoutahi, R. Ghahary and N. Taghavinia, *Rsc Adv*, 2014, 4, 45174-45179.
15. M. Q. Israr, J. R. Sadaf, L. L. Yang, O. Nur, M. Willander, J. Palisaitis and P. O. A. Persson, *Appl Phys Lett*, 2009, 95, 073114.
16. G. W. She, X. H. Zhang, W. S. Shi, X. Fan and J. C. Chang, *Electrochem Commun*, 2007, 9, 2784-2788.

17. M.-H. Zhao, Z.-L. Wang and S. X. Mao, *Nano Lett*, 2004, 4, 587-590.
18. Y. Xi, J. Song, S. Xu, R. Yang, Z. Gao, C. Hu and Z. L. Wang, *J Mater Chem*, 2009, 19, 9260-9264.
19. F. Li, C. W. Zhang, P. J. Wang and P. Li, *Appl Surf Sci*, 2012, 258, 6621-6626.
20. J. Yan, X. S. Fang, L. D. Zhang, Y. Bando, U. K. Gautam, B. Dierre, T. Sekiguchi and D. Golberg, *Nano Lett*, 2008, 8, 2794-2799.
21. X. Y. Kong, Y. Ding, R. Yang and Z. L. Wang, *Science*, 2004, 303, 1348-1351.
22. W.-Z. Wang, B.-Q. Zeng, J. Yang, B. Poudel, J. Huang, M. J. Naughton and Z. Ren, *Adv Mater*, 2006, 18, 3275-3278.
23. Z. L. Wang, R. Yang, J. Zhou, Y. Qin, C. Xu, Y. Hu and S. Xu, *Materials Science and Engineering: R: Reports*, 2010, 70, 320-329.
24. R. Yousefi and B. Kamaluddin, *Appl Surf Sci*, 2009, 255, 9376-9380.
25. G. Li, B. Wang, Y. Liu, T. Tan, X. Song and H. Yan, *Appl Surf Sci*, 2008, 255, 3112-3116.
26. Z. Z. Shao, L. Y. Wen, D. M. Wu, X. F. Wang, X. A. Zhang and S. L. Chang, *J Phys D Appl Phys*, 2010, 43.
27. H. Fujisawa, Y. Imi, S. Nakashima, M. Shimizu, Y. Kotaka and K. Honda, *J Appl Phys*, 2012, 112, 034111.
28. V. A. Antohe, M. Mickan, F. Henry, R. Delamare, L. Gence and L. Piraux, *Appl Surf Sci*, 2014, 313, 607-614.
29. B. Yin, Y. Qiu, H. Q. Zhang, J. Y. Ji and L. Z. Hu, *Crystengcomm*, 2014, 16, 6831-6835.
30. L. M. Yu, J. S. Wei, Y. Y. Luo, Y. L. Tao, M. Lei, X. H. Fan, W. Yan and P. Peng, *Sensor Actuat B-Chem*, 2014, 204, 96-101.
31. Z. Yan and L. Y. Jiang, *J Phys D Appl Phys*, 2011, 44, 365301.
32. Z. X. Zhang, L. F. Sun, Y. C. Zhao, Z. Liu, D. F. Liu, L. Cao, B. S. Zou, W. Y. Zhou, C. Z. Gu and S. S. Xie, *Nano Lett*, 2008, 8, 652-655.
33. M. C. Newton and R. Shaikhaidarov, *Appl Phys Lett*, 2009, 94, 153112.
34. Y. Ding, Z. L. Wang, T. J. Sun and J. S. Qiu, *Appl Phys Lett*, 2007, 90, 153510.
35. D. Gedamu, I. Paulowicz, S. Kaps, O. Lupan, S. Wille, G. Haidarschin, Y. K. Mishra and R. Adelung, *Adv Mater*, 2014, 26, 1541-1550.
36. Y. Lei, N. Luo, X. Q. Yan, Y. G. Zhao, G. Zhang and Y. Zhang, *Nanoscale*, 2012, 4, 3438-3443.
37. Y. D. Gu, J. Zhou, W. Mai, Y. Dai, G. Bao and Z. L. Wang, *Chem Phys Lett*, 2010, 484, 96-99.
38. N. Coppede, M. Villani, R. Mosca, S. Iannotta, A. Zappettini and D. Calestani, *Sensors-Basel*, 2013, 13, 3445-3453.
39. K. Sun, J. J. Qi, Q. Zhang, Y. Yang and Y. Zhang, *Nanoscale*, 2011, 3, 2166-2168.
40. M. C. Newton, S. Firth and P. A. Warburton, *Ieee T Nanotechnol*, 2008, 7, 20-23.
41. G. Zhu, A. C. Wang, Y. Liu, Y. S. Zhou and Z. L. Wang, *Nano Lett*, 2012, 12, 3086-3090.
42. K. Lefki and G. J. M. Dormans, *J Appl Phys*, 1994, 76, 1764-1767.
43. C.L. Sun, J.A. Shi, X.D. Wang, *J Appl Phys*, 2010, 108 034309
44. R. Araneo and C. Falconi, *Nanotechnology*, 2013, 24, 265707-265720.
45. B. Kumar and S. W. Kim, *Nano Energy*, 2012, 1, 342-355.

Figure Captions

Fig.1. Calculated piezopotential distributions for a ZnO nanotetrapod and a hexagonal nanorod. (a) and (c) are side and top views (at $L_T = 15\mu\text{m}$, the total height of the ZNT is $20.8\mu\text{m}$) of the piezopotential in the ZnO nanotetrapod, respectively. (b) and (d) are side and top views ($L_h = 20.8\mu\text{m}$) of the potential in the hexagonal nanorod, respectively.

Fig.2 The schematic plans of the designed sensors based on (a) ZHNR and (b) ZNT

Fig.3 The calculated piezopotential distributions in the ZNTs bent by a force (80nN) from different directions are revealed and viewed from the top.

Fig.4 Piezopotentials as a function of force, length and edge of nanotetrapods or hexagonal nanorods. (a)-(c) with a lateral force, (d) and (f) with a vertical compression force. Edge is $0.6\mu\text{m}$ in (a), (c),(d) and (f). Force is 80nN in (b), (c), (e) and (f). Length is $15\mu\text{m}$ in (a),(b), (d), and (e).

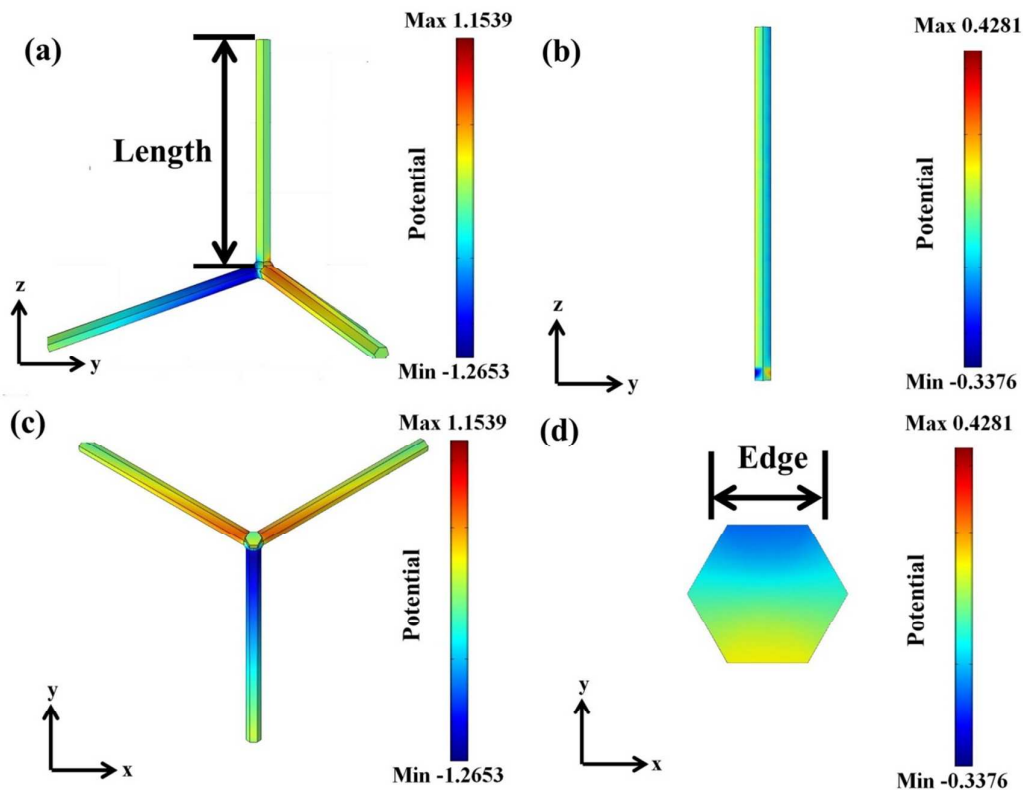


Fig.1. Calculated piezopotential distributions for a ZnO nanotetrapod and a hexagonal nanorod. (a) and (c) are side and top views (at $L_T = 15\mu\text{m}$, the total height of the ZNT is $20.8\mu\text{m}$) of the piezopotential in the ZnO nanotetrapod, respectively. (b) and (d) are side and top views ($L_h = 20.8\mu\text{m}$) of the potential in the hexagonal nanorod, respectively.

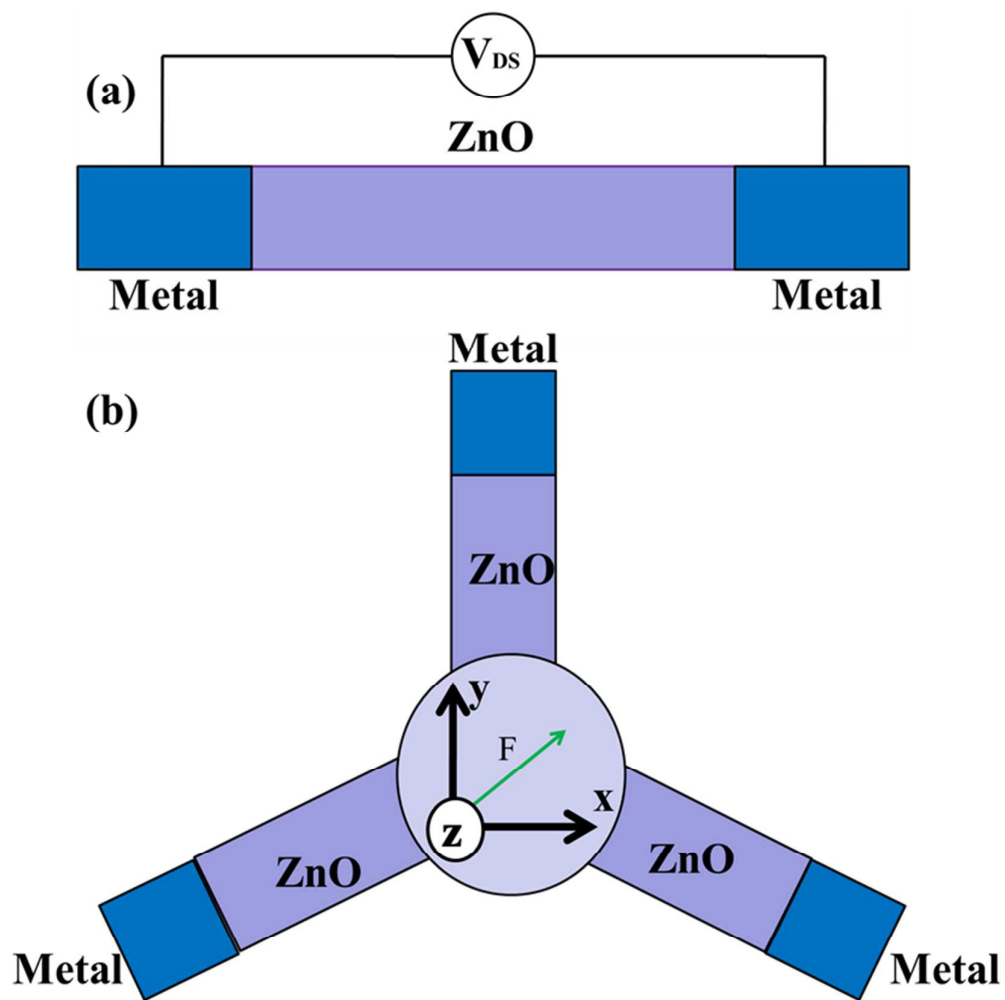


Fig.2 The schematic plans of the designed sensors based on (a) ZHNR and (b) ZNT

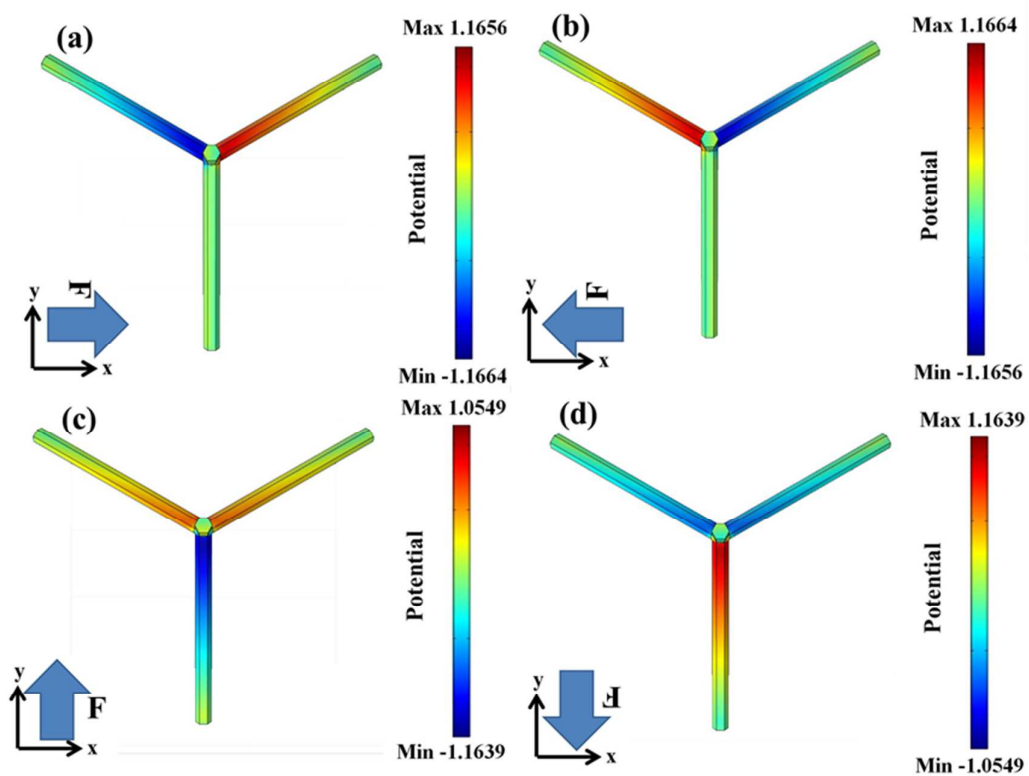


Fig.3 The calculated piezopotential distributions in the ZNTs bent by a force(80nN) from different directions are revealed and viewed from the top.

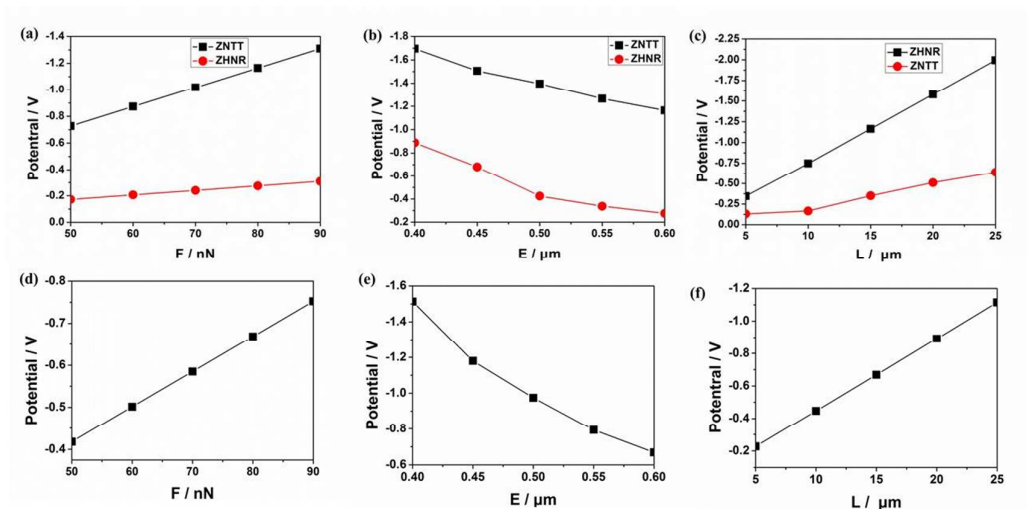


Fig.4 Piezopotentials as a function of force, length and edge of nanotetrapods or hexagonal nanorods. (a)-(c) with a lateral force, (d) and (f) with a vertical compression force. Edge is $0.6\mu\text{m}$ in (a), (c),(d) and (f). Force is 80nN in (b), (c), (e) and (f). Length is $15\mu\text{m}$ in (a),(b), (d), and (e).